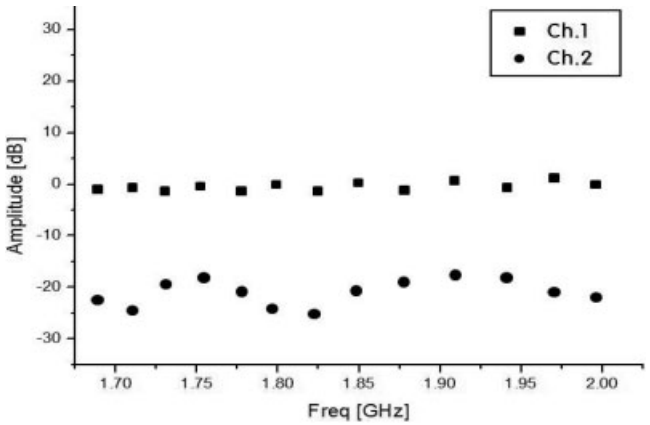

Figure 10 Measured insertion loss characteristics of dual directional coupler

$$Z_{oo}^{a} = \frac{1}{v_{Po}C_{o}^{a}} = \frac{1}{v_{Po}(C_a + C_{ab})}$$

$$Z_{oe}^{b} = \frac{1}{v_{Pe}C_{e}^{b}} = \frac{1}{v_{Pe}C_b}$$

$$Z_{oo}^{b} = \frac{1}{v_{Po}C_{o}^{b}} = \frac{1}{v_{Po}(C_b + 2C_{ab})}$$

We needed to simulate the structure illustrated in Figure 4 and this required divided line of b as can be seen in Figure 5.

4. EXPERIMENTAL RESULTS

For verifying theoretical results that previously described, we employed HFSS (High Frequency Simulating System) simulator providing high resolution and ease of mesh allocation. Figure 6 shows the microstrip prototype. In addition, tables below inform the respected simulation factors and results. Figures 7–10 show the experimental results that have been extracted; as can be seen, proposed dual directional coupler provides assymetric coupling and isolation values at a satisfactory rate.

5. CONCLUSION

It is essential to use dual directional coupler or other applications that also exhibit multiple advances to gain the various and dense advantages. These can be the much wider frequency bands, applicable coupling value whether if asymmetrically or not, precise values of desired parameters by users and so forth. In case of asymmetric value, which can be used for directing particular communication signal path, it definitely requires us to derive each impedance network. A normal 4-port directional coupler's mathematic function calculations were performed to practically apply it for designing 6-port dual directional coupler by multiple division methods. In our experimental results, we obtained much higher values of 45 and 38 dB of directivity characteristics, respectively. And we can demonstrate that these research works will provide various applicable advances such as dual mode antenna or other ancillary microwave component designs in foreseeable future.

ACKNOWLEDGMENT

This work was supported by the MIC (Ministry of Information and Communication), Korea, under the ITRC (Information Technology Research Center) support program supervised by the IITA (Institute of Information Technology Advancement) (IITA-2006-(C1090–0602-0011)).

REFERENCES

1. J.A.G. Malherve, Microwave transmission line couplers, Artech House, Norwood, MA, 1988.
2. G.L. Matthaei, L. Young, and E.M.T. Jones, Microwave filters, impedance matching networks and coupling structures, Artech House, Norwood, MA, 1980, pp. 218–228.
3. D.M. Pozar, Microwave and RF wireless systems, Wiley, New York, NY, 2002.
4. J.-S. Hong and M.J. Lancaster, Microstrip filters for RF/microwave applications, Wiley-Interscience, New York, NY, 2001.

OPTICAL CURRENT SENSOR BASED ON METAL COATED HI-BI FIBER LOOP MIRROR

B. V. Marques,[1,2] O. Frazão,[1] S. Mendonça,[1,3] J. Perez,[1] M. B. Marques,[1,3] S. F. Santos,[2] and J. M. Baptista[1,4]
[1] INESC Porto, Rua do Campo Alegre 687, 4169-007 Porto, Portugal; Corresponding author: ofrazao@inescporto.pt
[2] ISEP, Rua Dr. António Bernardino de Almeida 431, 4200-072 Porto, Portugal
[3] Department de Física, Fac. de Ciências, University do Porto, Rua do Campo Alegre 687, 4169-007 Porto, Portugal
[4] Department de Matemática e Engenharias, Universidade da Madeira, Campus da Penteada, 9000-390 Funchal, Portugal

Received 14 August 2007

ABSTRACT: *An optical current sensor based on a metal coated Hi-Bi fiber loop mirror is reported. This current sensor quantifies the current through the measurement of the temperature which varies accordingly with the magnitude of the electrical current. The temperature change is analyzed through the variation of the wavelength shift of a fringe minimum of a Hi-Bi fiber loop mirror. The minimum current detection was found to be approximately 10 A.* © 2008 Wiley Periodicals, Inc.
Microwave Opt Technol Lett 50: 780–782, 2008; Published online in Wiley InterScience (www.interscience.wiley.com). DOI 10.1002/mop.23217

Key words: *fiber optic sensor; optical current sensor; hi-bi fiber loop mirror*

1. INTRODUCTION

In specific industrial environments (i.e., where electrical current based systems are considered potentially dangerous for human physical integrity or where there is highly contaminated electromagnetic spectrum) optical current sensors are preferred instead of the traditional electrical ones, which are based on the Faraday or other magnetic effects [1-3]. Optical current sensors based on the Faraday effect are built with a silica fiber coil around the current conductor. This approach has some disadvantages like the extrinsic birefringence due to the bending of the coil, which decreases the current sensitivity. Moreover, vibrations induce linear birefringence and temperature variation influences the Verdet constant of the Faraday material compromising the performance of a simple sensor. Therefore, these cross sensitivities limit the implementation of simple practical applications of the Faraday effect, requiring alternative methods that increase the sensor complexity and cost [4]. In this article, it is presented a current sensor based on a wavelength shift of a fringe minimum of a high-birefringence

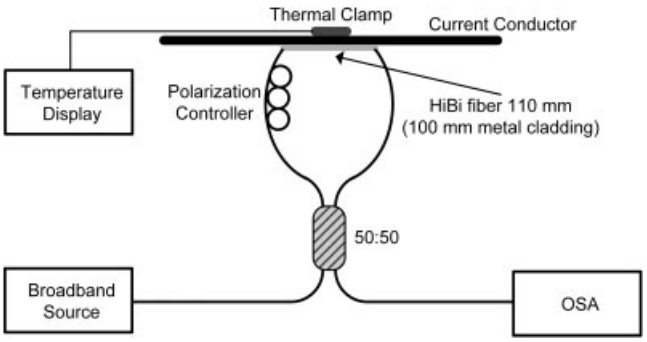

Figure 1 Schematic diagram of the experimental setup of the Hi-Bi FLM

(Hi-Bi) fiber loop mirror (FLM) resulting of the thermal response of the metal current conductor. It is demonstrated, theoretically and experimentally, one way to measure electrical current based on the variation of the conductor's temperature. The sensor head is a segment of Hi-Bi fiber, coated with a thin metallic layer, which support system is a FLM. The metal coating is used to allow a homogeneous thermal coupling between the fiber and the electrical current conductor.

2. PRINCIPLES

When a FLM that incorporates a Hi-Bi fiber, which is subject to temperature variation (ΔT), a well defined variation in the wavelength response ($\Delta\lambda$) of the interference pattern fringes occurs as it can be seen in the literature [5]. The relationship between $\Delta\lambda$ and ΔT is given by Eq. (1):

$$\Delta\lambda = \frac{\lambda_p}{l(n_e - n_o)}[lC_{T2} + (n_e - n_o)C_{T1}]\Delta T, \tag{1}$$

where, C_{T1} and C_{T2} are the fiber thermal expansion and thermal-optic coefficients, l the Hi-Bi fiber length, $n_e - n_o$ the birefringence index, and λ_p the operation wavelength.

Based on the Law zero of the Thermodynamics it is expected a thermal equilibrium between two bodies with different temperatures, for that reason the heat transfer phenomena is a transitory regime ($\lim_{t\to\infty}\frac{dT}{dt} = 0$).

This process depends on the material's mass (m) and specific heat capacity (c). The energy transfer with the time is translated in a Joule power loss (P) in the electrical resistance (R) with the cross of the current (I), as we can see in $P = R\,I^2$. The Joule power loss given by the dissipation of heat over the resistance, varies with the difference between the room temperature (T_a) and the system's temperature (T) and also the system respective thermal resistance (R_{th}), during the transitory regime:

$$P = m\,c\frac{dT}{dt} + \frac{T - T_a}{R_{th}}. \tag{2}$$

Because of the fact of only being considered the stationary regime, which is the regime where temperature is steady, the term relative to the transitory regime can be neglected ($dT/dt = 0$). This way and substituting P by $R\,I^2$, comes:

$$R\,I^2 = \frac{T - T_a}{R_{th}}, \tag{3}$$

where the thermal resistance R_{th} is given by the sum of R_{th1} and R_{th2}, the thermal resistance of conductor's material and the thermal resistance of the optical fiber coated with a thin metallic layer. These thermal resistances depend on thickness (e), thermal conductivity (δ) and thermal contact surface (s): $R_{th} = e/\delta\,s$). Taking into account the temperature dependence of the material resistance ($R = R_0\,(1 + \alpha(T - T_a))$) it can be obtained an expression for the temperature variation (ΔT) given by:

$$\Delta T = \frac{R_0 I^2}{k - \alpha R_0 I^2}, \tag{4}$$

where R_0 is the material resistance at room temperature (T_a), α the temperature coefficient of resistance, and k the inverse of R_{th}. The expression relates the temperature variation (ΔT) of the electrical current conductor with the direct variation of the electrical current (I).

Finally, substituting Eq. (4) in (1), it is obtained a relation between the wavelength variation of a fringe minimum ($\Delta\lambda$) and the electrical current (I):

$$\Delta\lambda = \frac{\lambda_p}{l(n_e - n_o)}[l\,C_{T2} + (n_e - n_o)C_{T1}]\frac{R_0 I^2}{k - \alpha R_0 I^2}. \tag{5}$$

3. EXPERIMENTAL RESULTS

Figure 1 shows a schematic representation of the experimental setup. It consists of an optical broadband source with the central wavelength of 1550 nm and bandwidth of 100 nm, a 3 dB coupler to form the FLM including the Hi-Bi metallic coated fiber segment attached to the current conductor. To improve the stability of the measurement, a homogeneous thermal coupling between the fiber and the electrical current conductor was performed applying a metal coating to the fiber. A Hi-Bi fiber segment was covered with a 300 nm Nikel-Cromium (80/20) layer. This layer was deposited at room temperature using an Edwards 306 evaporator, with a vacuum condition of 6×10^{-6} mbar and a constant current of $\approx$20 A to achieve a deposition rate of 0.5 nm/s.

The metallic coated Hi-Bi fiber segment, with a length of 100 mm, was fixed to the current conductor with epoxy glue and a thermal clamp was used to control de conductor's temperature. The spectral analysis was performed by an optical spectrum analyzer (OSA) with a resolution of 1 nm.

Figure 2 shows the Hi-Bi fiber loop mirror experimental response, which acts as a band pass filter for the input signal from the source [5-6]. The difference between the optical paths, introduced by the Hi-Bi fiber segment, for the two counter propagating waves

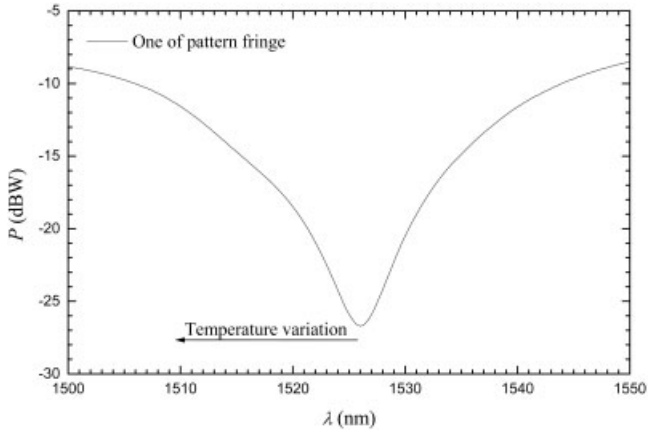

Figure 2 Spectral response of the Hi-Bi FLM

coming from the coupler as they transverse the loop results in constructive and destructive interference pattern. The experience was made with a 110 mm (l) PANDA Hi-Bi fiber segment with a birefringence index of 3.3×10^{-4}. This fiber length is 10 mm longer than the metal cladding to make possible the splices within the loop, splitting 5 mm for each side of the metal coating.

The copper current conductor used had the intrinsic values of 85.2 $\mu\Omega$, 1.5 mm, and 401 W/(m K), for electrical resistance over room temperature, material thickness and thermal conductivity, respectively. The sensor head composed by fiber and metal cladding had intrinsic values of -3.47×10^{-7}/°C, 1.1×10^{-6}, 1.1×10^{-6}, 125 μm, and 14.75 W/(m K) for thermal-optic coefficient (C_{T2}), thermal expansion coefficient (C_{T1}), temperature coefficient of resistance (α), thickness (e), and thermal conductivity (δ), respectively. The thermal contact surface between the materials was about 12.5 mm^2. The electrical current under measurement was in the range of 100–700 A. For each step of input current from the electrical source, the conductor's wavelength variation of one fringe minimum and the conductor's current were obtained as shown in Figure 3. The correspondent wavelength response had a nonlinear relationship with the current variation [in accordance to Eq. (5)]. This effect is due to the thermal response of the optical fiber. In other words, when heat is applied to a fiber with an index of birefringence obtained through stress over the core (SAP's – *Stress Applying Parts*), it results in a nonlinear response of the wavelength variation of the FLM fringe minima.

The sensitivity of the wavelength variation of fringe minimum as a function of the conductor's current can be divided into two regions. One region for lower current values (0–300 A) where the sensitivity is approximately -0.046 ± 0.005 nm/A and the other for higher current values (300–700 A) where the sensitivity is higher (approximately -0.146 ± 0.005 nm/A).

In order to obtain the minimum value of detected current, a 50 A step current was applied. Figure 4 shows the electrical current response over time of the sensor head. Based on the aforementioned result the minimum current detection could be quantified ($\delta I = 2\,\Delta I \sim 10$ A), where ΔI is the maximum current fluctuation interval for a constant conductor's current.

4. CONCLUSION

An optical current sensor based on a Hi-Bi fiber loop mirror was demonstrated with a sensitivity of -1.73 nm/°C. Because of nonlinear response between current as function of wavelength, the current sensitivity can be divided in two regions. For low current the sensitivity is -0.046 nm/A and for high current the sensitivity is three orders of magnitude higher (-0.146 nm/A). With this system, the minimum electrical current detection is approximately 10 A. The use of a fiber with metal coating allows homogeneous thermal coupling between the fiber and the electrical current conductor, improving the stability of the measurement. Nevertheless, this sensor requires the measurement of the room temperature. This sensor measures the true *rms* current value and can be an alternative solution to measure electrical current.

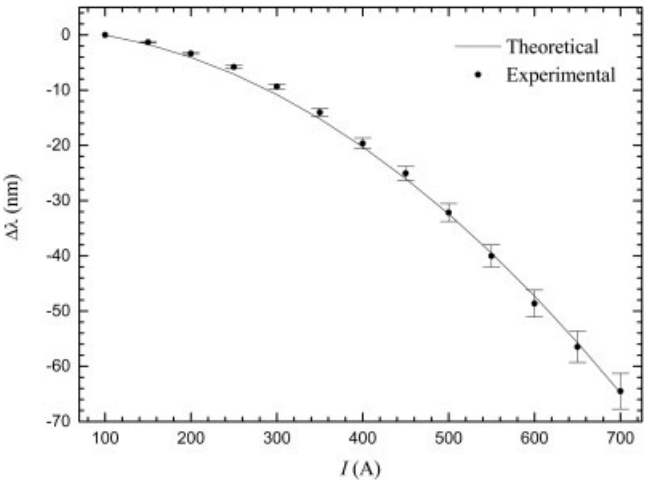

Figure 3 Theoretical and experimental wavelength variation responses as function of current

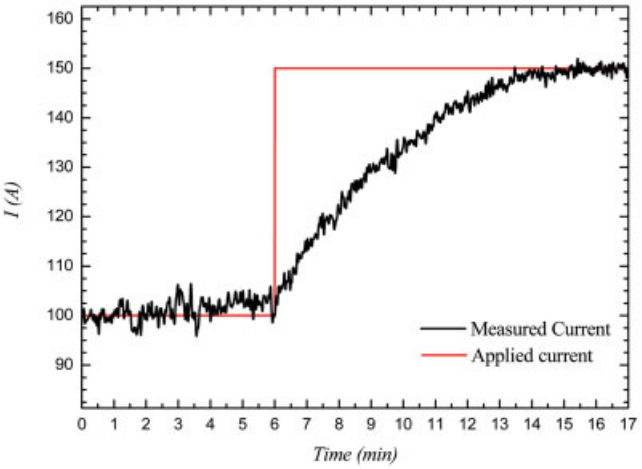

Figure 4 Current sensor response to a current step of 50 A. [Color figure can be viewed in the online issue, which is available at www.interscience.wiley.com]

REFERENCES

1. K. Bohnert, P. Gabus, J. Kostovic, and H. Brändle, Optical fiber sensors for the electric power industry, Opt Lasers Eng 43 (2005), 511-526.
2. P.-A. Nicati and P. Robert, Stabilized Sagnac optical fiber current sensor using one phase and two amplitude modulations, Optical Fiber Sensors Conference, 1992, pp. 402-405.
3. P.-A. Nicati and P. Robert, Stabilised current sensor using Sagnac interferometer, J Phys E Sci Instrum 21 (1988), 791-796.
4. P. Menke and T. Bosselmann, Temperature compensation in magnetooptic AC current sensors usingan intelligent AC-DC signal evaluation, J Lightwave Technol 13 (1995), 1362-1370.
5. Y. Liu, B. Liu, X. Feng, W. Zhang, G. Zhou, S. Yuan, G. Kai, and X. Dong, High-birefringence fiber loop mirrors and their applications as sensors, Appl Opt 40 (2005), 2382-2390.
6. X. Ma, G. Kai, Z. Wu, H. Guo, Y. Liu, S. Yuan, and X. Dong, Study of polarization independence for high birefringence fiber Sagnac interferometers, Microwave Opt Technol Lett 46 (2006), 183-185.